ELECTRON BEAM DYNAMICS IN THE DARHT-II LINEAR INDUCTION ACCELERATOR*

Carl Ekdahl, E. O. Abeyta, P. Aragon, R. Archuleta, G. Cook, D. Dalmas, K. Esquibel, R. Gallegos, R. Garnett, J. Harrison, J. Johnson, E. Jacquez, B. Trent McCuistian, N. Montoya, S. Nath, K.Nielsen, D. Oro, L. Rowton, M. Sanchez, R. Scarpetti, M. Schauer, G. Seitz, V. Smith, and R. Temple, LANL, Los Alamos, NM 87545, USA

H. Bender, W. Broste, C. Carlson, D. Frayer, D. Johnson, C. Y. Tom, C. Trainham, and J. Williams, NSTec, Los Alamos, NM 87544, USA

B. Prichard and M. Schulze, SAIC, San Diego, CA 92121, USA

T. Genoni, T. Hughes, and C. Thoma, Voss Scientific, Albuquerque, NM 87108, USA

Abstract

The DARHT-II linear induction accelerator (LIA) accelerates a 2-kA electron beam to more than 17 MeV. The beam pulse has a greater than 1.5-microsecond flattop region over which the electron kinetic energy is constant to within 1%. The beam dynamics are diagnosed with 21 beam-position monitors located throughout the injector, accelerator, and after the accelerator exit, where we also have beam imaging diagnostics. We discuss the tuning of the injector and accelerator, and present data for the resulting beam dynamics. We discuss the tuning procedures and other methods used to minimize beam motion, which is undesirable for its application as a bremsstrahlung source for multi-pulse radiography of explosively driven hydrodynamic experiments. We also present beam stability measurements, which we relate to previous stability experiments at lower current and energy.

INTRODUCTION

The 2-kA, 17-MeV DARHT-II linear induction accelerator (LIA) is unique in that its beam pulse has a long, 1.6-μs flattop during which the kinetic energy varies by less than ±1%. A kicker cleaves four short pulses out of this long pulse, and these are converted to bremsstrahlung for multi-pulse flash radiography of high explosive driven hydrodynamic experiments.

The long-pulse 2-kA beam is produced in a 2.5-MV diode. A diverter switch (crowbar) is incorporated to shorten the 2-μs flat-top pulse to as little as 200 ns flat-top (Fig. 1). After leaving the diode, the beam is accelerated by six induction cells to ~3.5 MeV, and then enters a transport zone designed to scrape off the long rise time, off-energy beam head. As in previous experiments [1,2,3], this beam-head clean-up zone (BCUZ) was configured to pass almost the entire beam head. The main LIA has 68 induction cells that have been upgraded to provide enough potential to accelerate the beam to more than 17 MeV. Each accelerating cell incorporates a solenoid to provide the focusing field for beam transport, as well as dipoles for beam steering.

The solenoids in the injector cells are tuned so that none of the off-energy electrons in the ~500-ns beam head are lost, even in the absence of accelerating fields. The solenoids through the main accelerator were tuned to transport a matched beam through a field increasing to more than 1 kG on axis to suppress beam breakup (BBU).

The tunes for the DARHT-II magnetic transport were designed with two envelope codes, XTR [4] and LAMDA [5]. These solve the beam-envelope differential equations keeping terms that are dropped from the usual paraxial approximation [6]. Initial conditions for XTR and LAMDA were provided by simulations of the space-charge limited diode using the TRAK gun-design code [7] and the LSP particle-in-cell code [8].

Non-invasive DARHT-II beam diagnostics, such as beam position monitors (BPM), are used on every shot [2,3]. Invasive diagnostics, such as a magnetic spectrometer and beam current profile imaging, are only occasionally used [1,2,9].

RESULTS

There was no loss of beam current through the LIA during the time that the accelerating cells were energized, as shown in Fig. 1, which is an overlay of beam current measurements though the injector and accelerator for a single shot. The ~7-MHz oscillation on the beam head is the result of large capacitances and inductances on the diode structure. The loss of some current in the beam head as it transited the BCUZ is evident. For these data, the current was terminated by the crowbar, which was timed to coincide with the end of the accelerating cell pulse. The red cursors in Fig. 1 delineate the 1.6-μs flattop used for the four radiography pulses. Slight beam loss in the BCUZ during the risetime is evident. Figure 2 shows the electron kinetic energy measured with our magnetic spectrometer. The kinetic energy of the accelerated beam exceeds 17.0 MeV for more than 1.6 μs. For this measurement five of the LIA cells were turned off, which reduced the energy by ~1.3 MeV from that expected with all 74 cells.

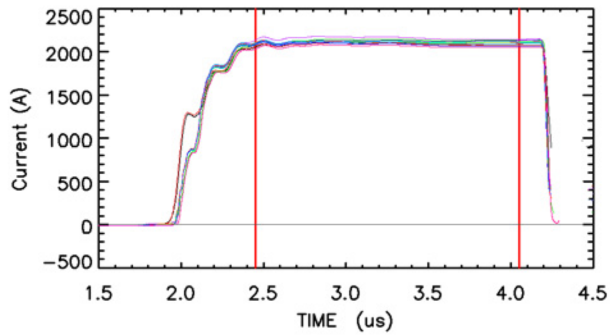

Figure 1: Overlay of beam current measurements in injector and accelerator. Red cursors indicate the 1.6-μs flattop region used for the four radiography pulses.

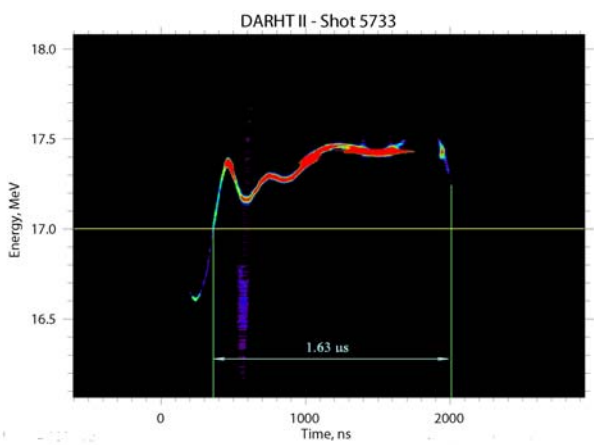

Figure 2: Magnetic spectrometer measurement of electron kinetic energy.

Low frequency beam motion at the exit of the accelerator was dominated by an energy dependent sweep. This sweep is undesirable because it effects the locations of the four radiography pulses, so we must understand it, and reduce its amplitude . While head-to-tail sweep is a characteristic of the resistive wall instability, we believe it unlikely that this instability is responsible for the sweep in DARHT-II. In a uniform strong solenoidal focusing field the distance for an initial perturbation to exponentiate is approximately $L = 3.1Ba^3/I_b/(\tau\rho)^{1/2}$, where a is the pipe radius in cm, B is the field in kG, I_b is the beam current in kA, τ is the pulse-length in μs, and ρ is the pipe resistivity in μΩ-cm [10]. Based on this theory, we estimate that the growth of an initial perturbation in DARHT-II is less than 60% over the length of the LIA. Moreover, in a strong solenoidal focusing field like DARHT-II the growth is independent of energy, in contradiction to our sweep data, which show a strong correlation with the energy variation illustrated in Fig. 2. The other likely cause of sweep is corkscrew, or the interaction of the energy-varying beam with a few accidental dipoles. Indeed, the observed sweep amplitude can be fit to a model of dipole deflection resulting from the observed energy variation (Fig. 3). Suppression of corkscrew by using steering dipoles has been demonstrated on other LIAs [11]. In an initial attempt to reduce our sweep amplitude, we used only a few of the available steering dipoles. We were able to reduce the sweep to an amplitude acceptable for commissioning the multi-pulse radiography target, and for our first radiographs of an upcoming hydrodynamic test. This initial attempt reduced the sweep amplitude by ~40% over the 1.6-μs flat top (Fig. 4). We anticipate further improvements in the future by using more of our dipoles.

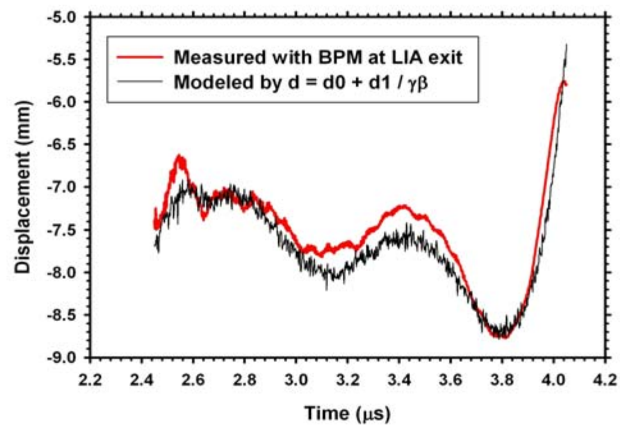

Figure 3: Comparison of measured sweep with model of sweep caused by beam energy variation interacting with a single accidental dipole.

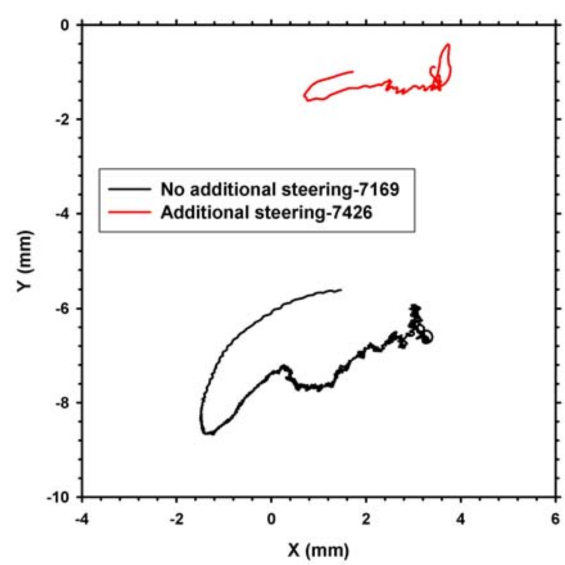

Figure 4: The beam sweep at the accelerator exit was reduced by using additional steering dipoles. Two different shots are shown. Black (lower): nominal steering. Red (upper): additional steering.

High-frequency motion due to low-amplitude BBU was observed at the accelerator exit [12]. For the DARHT-II LIA parameters theory predicts that the BBU amplitude saturates at $\xi(z)=(\gamma_0/\gamma)^{1/2}\xi_0\exp(\Gamma_m)$, where subscript zero denotes initial conditions, and γ is the usual relativistic mass factor, and $\Gamma_m = I_b N_g Z_\perp \langle 1/B \rangle / 3\text{x}10^4$ [13]. Here I_b is the beam current in kA, N_g is the number of gaps, the transverse impedance $Z_\perp$ is in Ω/m, and the average focusing force $\langle 1/B \rangle$ is in kG^{-1}. This theoretical prediction was confirmed in earlier experiments with legacy cells [3], and those results were used to design a tune with magnetic field strong enough to suppress the BBU to amplitude small enough that it did not significantly affect the measured radiographic spot size [15]. The observed BBU with this tune agrees with the earlier measurements and with this theory as shown in Fig. 5.

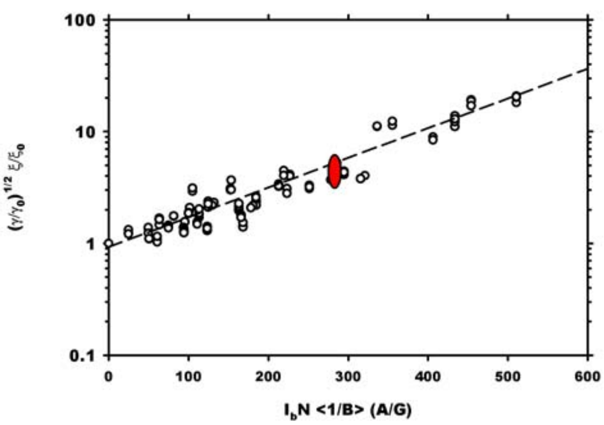

Figure 5: BBU growth in DARHT-II. Open circles: data obtained in low-current, low-energy experiments with legacy cells [3]. Filled oval: range of data obtained during commissioning the 2-kA, 18-MeV accelerator incorporating upgraded cells. The dashed line corresponds to the transverse impedance of the legacy cells.

In conclusion, we have now operated the DARHT-II accelerator at its fully rated current, energy, and pulse width. Even at the full 2-kA current, the solenoidal magnetic field of the tune was strong enough to suppress the BBU to acceptable amplitude. After some additional steering to reduce the sweep, the beam was stable enough for us to proceed with commissioning the multi-pulse kicker and bremsstrahlung converter for radiography.

This work was supported by the US National Nuclear Security Agency and the US Department of Energy under contract W-7405-ENG-36.

REFERENCES

[1] Carl Ekdahl, et al., “First beam at DARHT-II,” in Proc. 2003 Part. Accel. Conf., (2003), pp. 558-562

[2] Carl Ekdahl, et al., “Initial electron-beam results from the DARHT-II linear induction accelerator,” IEEE Trans. Plasma Sci. 33, (2005), pp. 892-900.

[3] Carl Ekdahl, et al., “Long-pulse beam stability experiments on the DARHT-II linear induction accelerator,” IEEE Trans. Plasma Sci. 34, (2006), pp.460-466.

[4] Thomas P. Hughes, David C. Moir and Paul W. Allison, “Beam injector and transport calculations for ITS,” in Proc. 1995 Part. Accel. Conf., (1995), pp. 1207-1209

[5] Thomas .P. Hughes, et al., “LAMDA User’s Manual and Reference”, Voss Scientific technical report VSL-0707, April 2007

[6] E. P. Lee and R. K. Cooper, “General envelope equation for cylindrically symmetric charged-particle beams,” *Part. Acc. 7*, (1976), pp. 83-95

[7] Stanley Humphries Jr., “TRAK – Charged particle tracking in electric and magnetic fields,” in Computational Accelerator Physics, R. Ryne Ed., New York: American Institute of Physics, (1994), pp. 597-601 .

[8] T. P. Hughes, R. E. Clark, and S. S. Yu, “Three-dimensional calculations for a 4 kA, 3.5 MV, 2 microsecond injector with asymmetric power feed,” Phys. Rev. ST Accel. Beams 2, (1999), pp. 110401-1 – 110401-6

[9] H. Bender, et al., “Quasi-anamorphic optical imaging system with tomographic reconstruction for electron beam imaging,” Rev. Sci. Instrum. 78, (2007), pp. 013301

[10] G. J. Caporaso, W. A. Barletta, and V. K. Neil, “Transverse resistive wall instability of a relativistic electron beam,” Particle Accelerators, vol. 11, 1980, pp. 71-79

[11] J. T. Weir, J. K. Boyd, Y.-J. Chen, J. C. Clark, D. L. Lager, and A. C. Paul, “Improved ETA-II accelerator performance,” in *Proc. 1999 Particle Accelerator Conf.*, New York, NY, March, 1999, pp. 3513-3515.

[12] Carl Ekdahl, et al., “Electron beam dynamics in the long-pulse, high-current DARHT-II linear induction accelerator,” in Proc. 2008 European Part. Accel Conf., (2008) pp. 968-970

[13] V. K. Neil, L. S. Hall, and R. K. Cooper, “Further theoretical studies of the beam breakup instability,” Particle Accelerators, vol. 9, 1979, pp. 213-222.

[14] R. Briggs and W. Waldron, “Transverse impedance measurements of the modified DARHT-2 accelerator cell design,” LBNL Report #59199, November, 2005

[15] Martin Schulze, et al., “Commissioning the DARHT-II Accelerator Downstream Transport and Target,” in Proc. 2008 Linear Accel. Conf. (these proceedings).